Accepted Manuscript

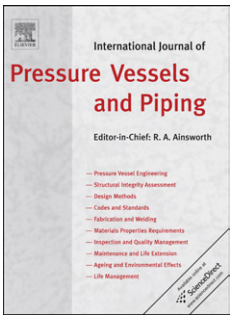

Numerical Simulation of Racheting and Fatigue Behaviour of Mitred Pipe Bends Under In-Plane Bending and Internal Pressure

H. Li, J. Wood, R. McCormack, R. Hamilton

PII: S0308-0161(12)00151-2

DOI: 10.1016/j.ijpvp.2012.11.003

Reference: IPVP 3253

To appear in: *International Journal of Pressure Vessels and Piping*

Received Date: 23 October 2011

Revised Date: 9 July 2012

Accepted Date: 28 November 2012

Please cite this article as: Li H, Wood J, McCormack R, Hamilton R, Numerical Simulation of Racheting and Fatigue Behaviour of Mitred Pipe Bends Under In-Plane Bending and Internal Pressure, *International Journal of Pressure Vessels and Piping* (2013), doi: 10.1016/j.ijpvp.2012.11.003.

Numerical Simulation of Racheting and Fatigue Behaviour of Mitred Pipe Bends Under In-Plane Bending and Internal Pressure

H. Li[a, b], J. Wood[a]*, R. McCormack[a], R. Hamilton[a]

[a] Department of Mechanical Engineering, University of Strathclyde, 75 Montrose Street, Glasgow G1 1XJ, UK

* Corresponding author.

[b] School of Mechanical Engineering and Automation, Zhejiang Sci-Tech University, Xiasha, Hangzhou 310018, China

Abstract

This paper investigates the ratcheting and fatigue behaviour of 90 degree single unreinforced mitred pipe bends subjected to a cyclic in-plane closing moment with a non-zero mean value and constant internal pressure. An experiment was conducted to induce ratcheting and low cycle failure of the mitred pipe bend. Material and structural response is considered both locally and globally using strain gauges at the locations of highest strain and also by measuring the displacement of the mitre end. These results along with the number of cycles to failure are compared with those produced from nonlinear finite element analysis. The predicted crosshead displacement from the multi linear model showed a good agreement with the test results. However, the finite element model failed to accurately replicate the strain level or trend from the tests, indicating the weakness of the material model used in simulating the cyclic hardening effect. It was also found that the FE models proposed were not able to model the final failure mode of the mitre due to the exclusion of crack simulation in the analysis, i.e. interaction between ratcheting and low cycle fatigue cracking was not considered in the idealised numerical model.

Keywords: Mitred pipe bend, Ratcheting, fatigue, finite element analysis

1. Introduction

Pressure components are often subjected to stresses greater than yield stress at discontinuities under normal operating conditions and this raises questions relating to the permissible level of yielding and also how the component responds under cyclic loading. If the maximum load in the cycle is lower than that to cause first yield, the response is wholly elastic and the structure may eventually fail by high-cycle fatigue. If the maximum load exceeds the static load carrying capacity of the structure, gross plastic deformation and plastic collapse will occur during the first load cycle. If the maximum load lies between yield and plastic collapse, either shakedown or an accumulation of plastic strains known as ratcheting can occur. Ratcheting leads to failure from incremental plastic collapse and must be avoided in pressure component design.

To date only one investigation has been made into the ratcheting behaviour of mitred pipe bends by Wood [1]. A large number of investigations have however been carried out into the cyclic plasticity and ratcheting behaviour which focuses on material ratcheting behaviour and its constitutive modelling, Rahman et al [2] Polizzotto [3], Chaboche [4]. Studies into the ratcheting-fatigue failure of smooth pipe bends subject to internal pressure are also well documented in literature Gupta et al [5] Oh et al [6], Abdalla et al [7].

Wood [8] conducted a review of mitred bend publications to date, referencing the structural behaviour of all types of mitred pipe bends. Post yield literature available discusses either limit or bursting pressure tests and collapse or limit bending moment tests, both in plane and out of plane or for a combination of pressure and moments. One publication, Vrillon et al [9] considered plastic behaviour including shakedown, when investigating other phenomena but to no great extent.

Neilson et al [10] compared experimental collapse loads of three mitres with finite element predictions for in plane closing of single unreinforced 90 degree mitred pipe bends. This publication is relevant as it considers mitres of identical material properties and geometry to those in the present investigation. Collapse loads from this investigation

were found to require an average force of 23.4KN. The FEA model using solid elements[11], large displacement analysis and a multilinear hardening material model replicated the average of three experimental tests within 1%. Using small displacements and an elastic perfectly plastic model, limit load simulations over predicted the maximum load for this configuration by approximately 43%. Clearly the inclusion of large displacements is important in capturing the weakening mechanism resulting from the ovalisation of the mitre.

Gresnigt [12] presented elastic and plastic results for various single mitres subjected to in-plane bending only and also pressure with in-plane bending. This publication focuses on applying analytical methods developed for smooth bends towards mitred bends. Ratcheting and shakedown effects were not considered, however within the cyclic load deflection graphs ratcheting is apparent although no comment is made to the phenomena or the purpose of the cycling.

Gupta, et al [5] investigated the ratcheting-fatigue relationship in smooth pipe bends subjected to internal pressure and cyclic bending by both experiment and FEA. The ratchet strain and non-relaxing mean stress was found to significantly reduce the low cycle fatigue life of the component. The analysis was conducted with the standard Chaboche model within the finite element program ANSYS and the authors found that deriving Chaboche material parameters from the monotonic stress strain curve simulated initial cycles well, whereas those derived from the cyclic stress strain curve simulated later cycles well. The authors concluded that inclusion of this transition in the material model would aid simulation accuracy.

Rahman, et al [2] considered seven cyclic plasticity material models for structural ratcheting response in FEA simulations. Models used were the Bilinear (Prager), Multilinear (Besseling), Chaboche, Ohno-Wang, Abdel Karim-ohno, modified Chaboche (Bari and Hassan) and modified Ohno-Wang (Chen and Jian). The first three material models are available in ANSYS, the others were customised material models implemented into ANSYS for the purpose of their study. The experimental response of straight steel pipes under cyclic bending with symmetric end rotation combined with steady internal pressure were recorded and compared with FEA results. None of the

models studied fully replicated the diameter change and circumferential strain ratcheting responses to a satisfactory level. Attempts were made to increase accuracy by conducting a detailed parameter sensitivity study for the Chaboche model on the parameters which influenced ratcheting simulations. After refining these parameters the results improved but the simulation was still not satisfactory. The authors concluded that anisotropy of materials and residual stresses were essential for advancement of low cycle fatigue predictions through simulations. The multilinear model was found to be the best overall, amongst the material models used, in simulating structural response, although it was still not accurate enough for fatigue life simulation and damage accumulation computation. The multi linear model accurately simulated the in-plane diameter change of one of the experiments, as well as strain responses. It was concluded that the customised material models were not any better than the standard models available in ANSYS in simulating local and global responses.

Wood, et al [1] conducted an experimental investigation into the ratcheting behaviour of a 90 degree single unreinforced mitred pipe bend subjected to a cyclic in plane closing moment with a non-zero mean value and constant internal pressure. Failure occurred due to a through thickness crack at a location 85° from the intrados of the mitred bend. Metallurgical analysis revealed overload from accrued plastic strain, therefore indicating a ratcheting contribution to failure. Ratcheting was also clear from the displacement and strain measurements. In the present paper, the structural response of the mitre geometry studied in [1] is further investigated using the finite element method.

2. Experiment

One bend specimen was arbitrarily selected from a total of seven "identical" bends that had been manufactured for a collapse and shakedown experimental programme. The dimensions of the specimen used in the experiment are show in Figure 1.

The test machine used a servo controlled hydraulic ram under load control to apply the load to the bottom of the mitred pipe bend. The pressure was increased to a value of 20MPa (which provides an equivalent straight pipe hoop stress of around half yield).

Two perpendicular strain gauge pairs were placed at two locations of high strain at the mitre intersection, as predicted by finite element analysis. The gauges where placed tangential and normal to the mitre intersection to align with the directions of principal strains. Further details of the experiment can be found in Wood et al[1].

FE Analysis

The model was created in ANSYS using the nominal sizes of the mitre specimens, as shown in Figure 1. Due to symmetry of geometry, material and loading, a quarter model was constructed. In addition to the symmetrical boundary conditions, a single node was prevented from moving in the vertical direction to prevent rigid body translation.

The finite element model used in this study has previously been validated by Neilson et al [10] for use in a comparison of plastic collapse and limit loads between experiment and FEA. The brick element SOLID186 with 20 nodes [11] was used throughout the model. This element accommodates the curved geometry of the model well and has a high order shape function. A finer mesh was used for current study at the bend intersection to compute accurate strain results for comparison with experiment and fatigue assessment, as shown in Figure 2.

Using solid elements will lead to elastic stress singularities at the mitre intersection as there is no fillet radius. As this is a plasticity solution no singularity will exist as yielding will blunt the singularity and result in load shedding to the surrounding material. The inclusion of non-linear geometry is not specified for ratcheting assessments based on elastic analysis within ASME VIII Div2 2010 section 5.5 [13], but is however specified in an elastic plastic analysis. For most pressure components non-linear geometry will not greatly affect the behaviour until the solution is post yield which would necessitate the use of an elastic-plastic analysis.

In the FE model, a constant internal pressure of 20MPa was applied to the inner surface of the model. The cyclic load of 15KN (30KN for the full model) was applied to the pin and then to the model through a contact pair between the pin and the lug. This allowed the pin to roll within the socket which produces a more accurate representation of the changing length of the moment arm as the bend closes. The pressure load was applied first and then the cyclic load from zero to test load level was applied.

Material Models and Properties

The mitred pipe bends were manufactured from cold finished seamless steel tubes as specified in B.S.I. specification for cold finished seamless steel tubes [14], with a tolerance on thickness of $\pm 10\%$ with a minimum of ± 0.1 mm and a tolerance of ± 0.30 mm on diameter. The nominal dimensions of the pipe are 100 mm dia. $\times$ 4mm thick.

A tensile test in accordance with reference [15] was carried out using specimens manufactured from the pipe. The values of Young's Modulus and Poisson's Ratio were obtained as 209 GPa and 0.27 respectively. The material Yield Stress was measured as 518 MPa at 2000micro-strain and the Ultimate Stress was 638MPa at 96,300 micro-strain.

The elongation and cross-section area at fracture were 16.14% and 1.16E-5m^2, respectively，based on which area reduction, true strain at fracture, fracture ductility and fracture strength were calculated. The summary of material properties used is presented in Table 1. Cyclic strength coefficient and cyclic strain hardening exponent were obtained through Equations (6-8) and also included in this table.

Table 1 – Material properties

Yield stress, $\sigma_{0.2}$	Young's modulus, E	Elongation	Area reduction	Fracture strength, σ_f
518MPa	209GPa	0.1614	62.13%	1110MPa
Strain at fracture	Fracture ductility, ε_f	Fracture ductility parameter, α	Cyclic strength coefficient, K'	Cyclic strain hardening exponent, n'
0.149626	0.970898	0.603178	1109.762MPa	0.11662

When modelling the plastic response of typical metals, two basic types of hardening can be defined: isotropic hardening (yield surface size change) and kinematic hardening (translation of the yield surface in stress space). The kinematic hardening is generally attributed to be the primary reason for ratcheting. The von Mises yield criterion for kinematic hardening material can be expressed as

$$f\left(\boldsymbol{\sigma}-\boldsymbol{\alpha}\right)=\left[\frac{3}{2}\left(\mathbf{s}-\mathbf{a}\right)\bullet\left(\mathbf{s}-\mathbf{a}\right)\right]^{1/2}=\sigma_0 \qquad (1)$$

Where, $\boldsymbol{\sigma}$ is the stress tensor and $\mathbf{s}$ is the deviatoric stress

tensor, $\boldsymbol{\alpha}$ is the current center of the yield surface, $\mathbf{a}$ is the current center of the yield surface in the deviatoric space, $\boldsymbol{\sigma}_0$ is the size of the yield surface (constant for a cyclically stable material), the kinematic hardening rule is given by:

$$d\mathbf{a} = g\left(\boldsymbol{\sigma}, \boldsymbol{\varepsilon}^p, \mathbf{a}, d\boldsymbol{\sigma}, d\boldsymbol{\varepsilon}^p, \text{etc}\right) \qquad (2)$$

Where, $\boldsymbol{\varepsilon}^p$ is the plastic strain tensor, for linear kinematic hardening model.

$$d\mathbf{a} = C d\boldsymbol{\varepsilon}^p \qquad (3)$$

Multilinear kinematic hardening can be seen as a piecewise linear kinematic hardening rule. In uniaxial loading, it essentially divides the stress-strain curve into many linear segments. Chaboche [16] proposed a `decomposed' nonlinear kinematic hardening rule in the form:

$$d\mathbf{a} = \sum_{i=1}^{n} d\mathbf{a}_i, \quad d\mathbf{a}_i = \frac{2}{3} C_i d\boldsymbol{\varepsilon}^p - \gamma_i \mathbf{a}_i dp, \quad dp = \left| d\boldsymbol{\varepsilon}^p \right| \qquad (4)$$

where, C_i and γ_i are material constants. For three-decomposed rules (n=3), the Chaboche model has three segments of a stable hysteresis loop. Bari [17] proposed a method to compute the Chaboche parameters C1, C2, C3 and γ_1, γ_2, γ_3, from a uniaxial strain-controlled stable hysteresis curve, which requires a cyclic tension-compression test. However, such test data was not available to the authors and the Chaboche parameters were derived instead from a cyclic stress-strain curve [18], which can be obtained from a tensile test [19].

The cyclic stress strain curve is expressed as

$$\frac{\Delta\varepsilon}{2} = \frac{\Delta\sigma}{2E} + \left(\frac{\Delta\sigma}{2K'}\right)^{\frac{1}{n'}} \qquad (5)$$

$$\frac{\Delta p}{2} = \left(\frac{\Delta\sigma}{2K'}\right)^{\frac{1}{n'}} \qquad (6)$$

where, $\Delta\sigma$ is stress range, $\Delta\varepsilon$ is strain range, Δp is the plastic strain range, K' is a cyclic strength coefficient and n' the cyclic strain hardening exponent, calculated using the following equations [19]:

$$K' = 57\left(\frac{\sigma_f \sigma_{0.2}}{\sigma_b} \varepsilon_f^{-h}\right)^{0.545} - 1220 \qquad (7)$$

$$n' = \frac{\sigma_{0.2}}{\sigma_f - \sigma_b} h \qquad (8)$$

$$h = \frac{\lg\left(\frac{\sigma_f^2}{\sigma_{0.2}\sigma_b}\right)}{2\lg\left(500\varepsilon_f\right)} \qquad (9)$$

where, $\sigma_{0.2}$ is yield strength, σ_f fracture strength,σ_b ultimate tensile strength and $\varepsilon_{0.2}$ the fracture ductility.

In 1-D, the cyclic stress strain curve can be expressed by a Chaboche model in the form of:

$$\frac{\Delta\sigma}{2} = \frac{C}{\gamma}\tanh\left(\gamma\frac{\Delta p}{2}\right) + \sigma_0 \qquad (10)$$

A least squares curve fitting approach is applied to a sample of stress-plastic strain range points ($\Delta\sigma$,Δp) evaluated from Equation (6) to determine C and γ. Assuming the Chaboche model with four backstresses, the computed C and γ are tabulated in Table 2.

Table 2 - Chaboche material model contstants

Backstresses	C, MPa	γ
1	4078	101.91
2	8083	101.91
3	2759	22.249
4	891.387	0.000107

The multilinear and Chaboche nonlinear kinematic models are plotted in Figure 3 along with the stress-strain curve from tensile test.

Results and Discussion

Failure mode of the mitre

The experiment was stopped when a through thickness crack caused oil to leak from the mitre and the pressure could no longer be maintained. The crack was located at the

expected location of highest plastic strain predicted by the FEA. The crack location lay perpendicular to the weld at approximately 85 degrees from the intrados of the mitre.

The mitre bend was sectioned along the symmetry plane normal to the mitre intersection for crack detection tests with dye penetrant on the inside and outside surfaces. The through thickness crack can clearly be seen on the left section of the mitre in Figure 4. Sections of the pipe containing the cracks were removed for metallurgical analysis of the crack face. Sections were then cut along SECTION L1 .

The through thickness crack perpendicular to the weld run, propagates from the outer surface. This is consistent with preliminary elastic FEA results showing the outer surface in tension and inner surface in compression at this location. The outer crack mouth, shown in Figure 4, showed clear evidence of plasticity, as illustrated by the elongation of weld grains. This would suggest plasticity as a contributing source of initial damage, leading to crack initiation and low cycle fatigue propagation, in addition to plastic strain accumulation due to ratcheting. A more detailed metallurgical analysis is available in Wood et al [1].

Displacement

The crosshead displacement history is presented in Figure 5. The blue line and green line represents the experimental maximum and minimum displacements in each cycle, respectively. A steady increase in the maximum crosshead displacement can be seen over the whole cyclic loading. Through thickness cracking occurred at the 181st cycle. As shown, towards the end of the experiment the returning position of the crosshead was observed to decrease, as the test progressed. It is believed that this could be due to a variable elastic follow up effect during the crack propagation.

The multi linear model has been shown to represent the structural response relatively well. However the Chaboche model is too stiff in that the predicted displacement is much lower than the experimental results. This lack of correlation is also apparent from the stress strain curves shown in Figure 3. The Chaboche model is well above the stress strain curve from the tensile test, indicating the inappropriateness of deriving the Chaboche model from the cyclic stress strain curve for the current application. The cyclic

stress strain curve is based on stabilized hysteresis loops of different strain ranges. It always takes a number of cycles of cyclic hardening for the hysteresis loop to stabilize. The cyclic hardening process has been ignored and only the stabilized stress strain data are included in the cyclic stress strain curve. However the mitre material experienced a cyclic hardening process and the stress strain curve should therefore be lower than that obtained from cyclic stress strain curve and higher than the monotonic stress strain curve from a tensile test. Thus cyclic material testing is required to accurately determine the hysteresis loop stabilization behaviour for the material. The range of plastic strain within the hysteresis loops during material testing should be similar to the range expected during the application. Such data is currently unavailable for the mitre material.

For finite element models, the curves shown in Figure 5 become flat after 20 cycles and no ratcheting failure has been found even after 800 cycles. When checking the displacement history during the 399^{th} and 400^{th} cycle, shown in Figure 6, it is clear that the mitre model had exhibited plastic shakedown behaviour. Therefore, the proposed FE models are not capable of predicting the actual mitre failure mode. This is mainly because the fatigue failure (crack propagation) is not simulated in the model.

Strain

In the test the strain gauge pair (strain gauge 1&2), located at 85° from intrados failed early , therefore the strain results cannot be presented for comparison with the finite element model. Strain gauge 4, from the other strain gauge pair (strain gauge 3&4), which was placed at 35° from intrados, recorded the strain along the mitre intersection.

The ratcheting behaviour is clearly illustrated in Figure 7 for the first 1500 seconds (20 cycles), after which both the strain range and maximum strain decreased in a number of stages. This is strong evidence that the material, adjacent to the strain gauge, experienced crack growth normal to strain gauge 4 and hence the strain experienced by the gauge reduced as the crack progressed. The finding is in line with the metallurgical analysis above, where through thickness cracks were found across the weld. This remarkable strain distribution is a clear illustration of the interaction of ratcheting (plastic strain

accumulation) and low cycle fatigue (crack growth). Therefore strain results are only compared with numerical predictions in the first few cycles, shown in Figure 8, since the finite element model didn't include the crack propagation simulation. It is clear that the finite element model overestimates the strain results for strain gauge 4. It should be noted that only numerical strain results from the finite element model with the multilinear material model are presented, as the Chaboche model could not accurately predict displacement as shown in the previous section.

Gauge 3 from the strain gauge pair (strain gauge 3&4), which was placed at 35°from intrados in the direction perpendicular to the mitre intersection, provided some indication of ratcheting only in the first two cycles. Due to the cyclic hardening effect, the absolute strain values exhibited a slight decrease with the number of cycles. However the numerical prediction didn't show this trend, indicating the weakness of the current multilnear finite element model in simulating the cyclic hardening effect, as shown in Figure 8. The predicted strain 3 curve also has a smaller strain range than the experiment. A slow ratcheting process can be seen for the first few cycles, and then the curve becomes steady with shakedown occuring. This is illustrated in Figure 9, where the equivalent strain curve and equivalent strain increment curve progress to be horizontal after a number of cycles.

As a result of plastic shakedown, the FE model would not exhibit the actual mitre failure mode and hence overestimates the number of cycles to failure.

Fatigue life assessment

A through thickness crack was the failure mode of the mitre, however in current FE models; the low cycle fatigue (crack propagation) process was not explicitly included. Strain-life equations are used in this section to estimate the fatigue life.

The classical Basquin-Coffin Manson (BCM) strain-life equation predicts the number of cycle to failure under an applied strain range only:

$$\frac{\Delta\varepsilon}{2} = \frac{\sigma_f'}{E}(2N)^b + \varepsilon_f'(2N)^c \qquad (11)$$

where b is the fatigue strength exponent, c is the fatigue ductility exponent, σ_f' is the fatigue strength coefficient and ε_f' fatigue ductility coefficient. The four-point method

was employed to evaluate the above four constants according to the procedure in ASM Metal Handbook [20], based on monotonic tensile data.

Table 3: Four fatigue constants in Basquin-Coffin Manson equation

Fatigue strength exponent, b	Fatigue strength coefficient, σ_f'	Fatigue ductility exponent, c	Fatigue ductility coefficient, ε_f'
-0.12949	1270 MPa	-0.5594	0.6532533

To consider the mean stress effect Morrow [21] modified the BCM strain -life equation by deducting σ_m from σ_f' . Further Manson and Halford [22] modified the strain-life equation to maintain the independence of the elastic-plastic strain ratio from mean stress and the modified equation is

$$\frac{\Delta\varepsilon}{2} = \frac{(\sigma_f' - \sigma_m)}{E}(2N)^b + \varepsilon_f'\left(\frac{\sigma_f' - \sigma_m}{\sigma_f'}\right)^{\frac{c}{b}}(2N)^c \qquad (12)$$

When considering the effect of ratchet strain and mean stress on fatigue life, equation (12) becomes [5]:

$$\frac{\Delta\varepsilon}{2} = \frac{(\sigma_f' - \sigma_m)}{E}(2N)^b + (\varepsilon_f' - \varepsilon_r)\left(\frac{\sigma_f' - \sigma_m}{\sigma_f'}\right)^{\frac{c}{b}}(2N)^c \qquad (13)$$

The damage calculation was carried out cycle by cycle and Miner's rule was used to obtain cumulative damage fraction and evaluated number of cycles to failure. In each cycle, the strain range and mean stress were calculated as per ASME VIII-2 section 5.5, Protection Against Failure From Cyclic Loading [13]. The evaluated mean stress, ratchet strain and strain range values at crack initiation location and as used in fatigue life prediction are presented in Figures 10-12 as function of cycles, respectively.

The number of cycles to failure from the Basquin-Coffin Manson equation (11) is 2695 and 84 from the modified equation (13). It clearly shows the substantial effect of ratchet strain on the fatigue life. From the experiment, as shown in Figure 7, a crack has already developed to a length at the 20th cycle sufficient to affect the strain gauge and the complete through thickness crack occurred at the 181st cycle. The predicted 84 cycles

falls between 20 and 181, which is reasonably close, given the complex failure mechanisms involved and lack of coupling of ratcheting and low-cycle fatigue in the FE model. The Basquin-Coffin Manson equation (11) significantly over predicts the number of cycles to failure, whereas the modified equation (13) gives a reasonable estimation of fatigue life.

Conclusion

A 90 degree single unreinforced mitred pipe bend under a cyclic in-plane closing moment and constant internal pressure was studied by both experiment and FE analysis. The mitre failed due to through-thickness leakage, as a result of ratcheting-fatigue interaction with the low cycle fatigue as the main contributor to failure. In the experiment, the accumulation of ratcheting strain exhausted the ductility and hence a crack initiated, propagated and caused leakage in a fewer number of cycles.

The finite element model proposed in this paper wasn't able to model the final failure mode of the mitre due to the exclusion of crack simulation in the FE analysis, i.e. interaction between ratcheting and low cycle fatigue cracking was not considered in the current idealised numerical model. Consequently, the FE model predicted a plastic shakedown behaviour rather than any form of cracking and failure. To estimate the fatigue life of the mitre based on FE results, two strain-life equations were used: Basquin-Coffin Manson equation and the modified equation considering the effect of mean stress and ratcheting. It was found that the Basquin-Coffin Manson equation over predicted the fatigue life while the modified equation provided a resonable estimation. To better predict the number of cycles to failure, an approach which implicitly includes crack initiation and damage progression, could be used.

The predicted crosshead displacement from the multi linear model showed a good agreement with the test results. However the FE model with Chaboche material model appeared too stiff, in that the predicted displacement was much lower than experimental results. This was due to the lack of test data for Chaboche model parameter determination. Instead the parameters were derived from a cyclic stress strain curve, which is based on

stabilized hysteresis loops of different strain ranges and hence over-predicted the strength of the mitre.

Only numerical strain results from the finite element model with a multilinear material model are compared with experimental results because of the Chaboche model derived from the cyclic stress strain curve not being able to predict displacements with any degree of accuracy. The finite element model was not capable of accurately replicating the strain level or trend from the tests, indicating the weakness of current multilnear finite element models in simulating the cyclic hardening effect. Therefore the Chaboche model containing both isotropic hardening and kinematic hardening is required to accurately simulate the strain history in the mitre. As future work, the parameters for such a Chaboche model can be determined using cyclic material testing whilst ensuring that the range of plastic strain within the testing is similar to the range expected during the application and analysis of the component.

References

1. Wood, J., McCormack, R. and Li, H., Experimental Investigation into the Ratcheting Behaviour of a 90 Degree Mitred Pipe Bend Under In-Plane Bending and Internal Pressure, submitted to the Journal of Strain Analysis for Engineering Design, October 2011.
2. Rahman S. M., Hassan T., Corona E., Evaluation of Cyclic Plasticity Models in Ratcheting Simulations of Straight Pipes Under Cyclic Bending and Steady Internal Pressure, International Journal of Plasticity, 24, 2008, pp1756-1791.
3. Polizzotto C., A Study on Plastic Shakedown of Structures: Part II - Theorems, ASME J. Appl. Mech., 60, pp318-330, 1993.
4. Mechanics of Solid Materials, J. Lemaitre and J.-L. Chaboche, Cambridge University Press ISBN 0 521 32853 5, 1990.

5. Gupta S.K., Goyal S., Bhasin V., Vaze K.K., Ghosh A.K. and Kushwaha H.S., Ratcheting-Fatigue Failure of Pressurized Elbows Made of Carbon Steel, Proceedings of SMiRT 20, Espoo, Finland, August 9-14 2009.

6. Oh C-S, Kim Y-J and Park C-Y, Shakedown Limit Loads for Elbows Under Internal Pressure and Cyclic In-plane Bending, Int. J. of Pressure Vessels and Piping, v85, Issue 6, pp 394-405, June 2008.

7. Abdalla H.F., Megahed M.M. and Younan M.Y.A., Determination of Shakedown Limit Load for a 90-Degree Pipe Bend Using a Simplified Technique, J. Pressure Vessel Technol., v128, Issue 4, November 2006.

8. Wood, J. A Review of Literature for the Structural Assessment of mitred pipe bends. International Journal of Pressure Vessels and Piping, v85, n5, pp275-294, 2008.

9. Vrillon, B., Roche, R. and Baylac, G. Comparison Between Experimental and Computer Analyses of the Behaviour Under Pressure of a 90^0 Bend with an Elliptical Section, 2nd Int. Conf. Press. Vess. Tech., San Antonio, Texas, 1-14 Oct. 1973.

10. Neilson R., Wood J., Hamilton R. & Li H., A Comparison of Plastic Collapse and Limit Loads for Single Mitred Pipe Bends Under In-Plane Bending. International Journal of Pressure Vessels and Piping, v87, pp550-580, 2010.

11. Ansys 11.0. Ansys Inc,. Canonsburg, PA, USA, 2007, http://www.Ansys.com/.

12. Gresnigt A.M., Elastic and Plastic Design of Mitred Bends, Proc. 12^{th} Int. Offshore and Polar Engineering Conf., Kitakyushu, Japan, May 26-31, 2002.

13. American Society of Mechanical Engineers, Boiler & Pressure Vessel design codes an international code, section VIII division 2 Rules for Construction of Pressure Vessels, Part 5 Design by Analysis Requirements, subsection 5, Protection Against Cyclic Loading, 2010.

14. B.S.I. specification for seamless and welded steel tubes for automobile, mechanical and general engineering purposes. Part 4: specific requirements for cold finished seamless steel tubes, BS 6323e4; 1982.

15. B.S.I. Tensile Testing of Metallic Materials: Method of Test at Ambient Temperature; BS EN 10002-1:2001.

16. Chaboche, J.L., Time-independent constitutive theories for cyclic plasticity, International Journal of Plasticity 2, 149-188, 1986.
17. Bari S, Hassan T, Anatomy of coupled constitutive models for ratcheting simulation. International Journal of Plasticity,16, pp.381–409, 2000.
18. Dewees D.J., Application of Elastic-Plastic Design Data in the New ASME B&PV Code Section VIII Division 2, Proceedings of the ASME 2010 Pressure Vessels & Piping Division / K-PVP Conference, PVP2010-25641, July 18-22, 2010, Bellevue, Washington, USA
19. Zhang, Z., Qiao, Y., Sun, Q., Li, C., Li, J., Theoretical Estimation to the Cyclic Strength Coefficient and the Cyclic Strain-Hardening Exponent for Metallic Materials: Preliminary Study, Journal of Materials Engineering and Performance, v18, Issue 3, pp.245-254, 2009.
20. ASM International, ASM Metals HandBook, v19 - Fatigue And Fracture, 1996.
21. Morrow, J., Fatigue properties of metals. In: Fatigue Design Handbook, Section 3.2, ed. J. A. Graham,Society of Automotive Engineers, Warrendale, PA, Vol. AE-4. 1968.
22. Manson, S. S. and Halford, G. R., Practical implementation of the double linear damage rule and damage curve approach for treating cumulative damage. International Journal of Fracture, Vol. 17. P. 169-172, 1981.

DIMENSION	SPECIMEN 5	FE MODEL
A (deg) 1	90.276	90
L1 (mm) 1	500.972	502.0
L2 (mm) 1	499.962	502.0
H1 (mm) 1	47.891	49.5
H2 (mm) 2	50.353	49.5
X (mm) 2	316.982	320
D (mm) 3	101.34 - 101.82	100
T (mm) 3	3.84 - 4.12	4
W1 (mm) 4	60	60
W2 (mm) 4	60	60
B (mm) 4	160	160
T1 (mm) 4	20	20
T2 (mm) 4	20	20
H3 (mm) 4	50	50
HD (mm) 4	20	20

1 Measured MITUTOYO coordinate measurement machine.

2 Derived. 3 Surveyed micrometer. 4 Nominal.